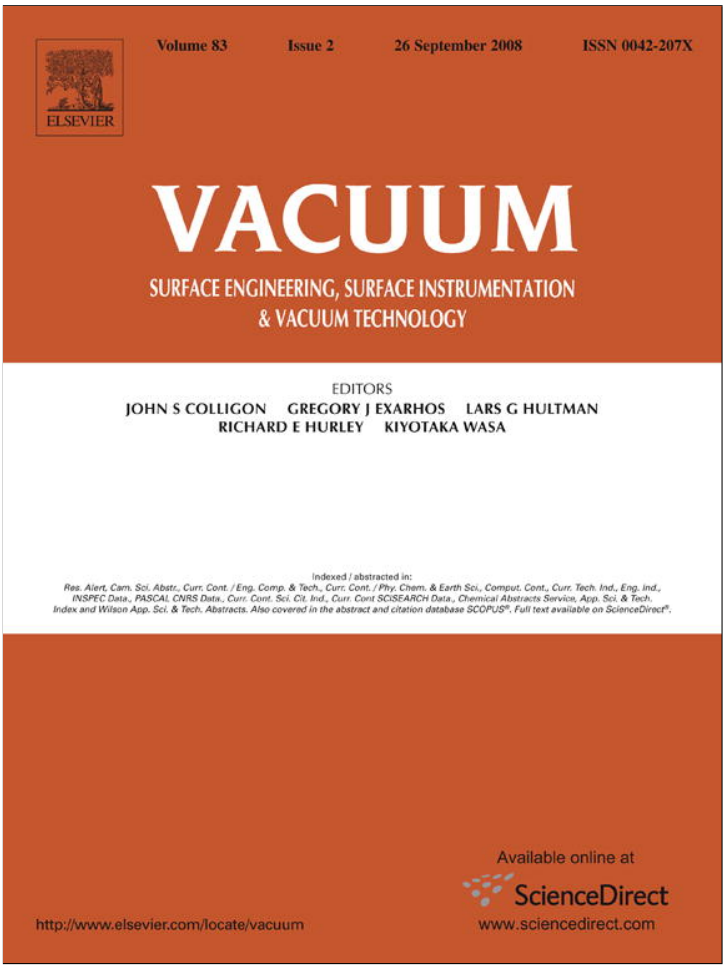

Vacuum 83 (2009) 302–307

Contents lists available at ScienceDirect

Vacuum

journal homepage: www.elsevier.com/locate/vacuum

Polymer pre-treatment by linear anode layer source plasma for adhesion improvement of sputtered TiN coatings

Juergen M. Lackner [a,*], Wolfgang Waldhauser [a], Manfred Schwarz [b], Leonard Mahoney [c], Lukasz Major [d], Boguslaw Major [d]

[a] Joanneum Research Forschungsgesellschaft mbH, Laser Center Leoben, Leobner Straße 94, A-8712 Niklasdorf, Austria
[b] Veonis Technologies GmbH, Junkersstraße 1, D-82178 Puchheim/München, Germany
[c] Veeco Instruments Inc., Veeco Ion Beam Equipment Group, 2330 E. Prospect, Fort Collins, CO 80525, USA
[d] Polish Academy of Sciences, Institute of Metallurgy and Materials Sciences, ul. Reymonta 25, 30-059 Kraków, Poland

ARTICLE INFO

Article history:
Received 30 May 2008
Accepted 23 June 2008

Keywords:
Coating of polymers
Titanium nitride
Room temperature magnetron sputtering
Plasma etching
Anode layer source
PA
PC
PET

ABSTRACT

The pre-treatment of work-piece surfaces is decisive for improved adhesion of tribological, decorative, sensor, biocompatible, etc. coatings subsequently deposited by vacuum coating techniques. Most current industrial techniques (mainly glow discharges) miss the requirements for activating temperature-sensitive and electrically insulating materials. Gridless plasma sources like the linear anode layer ion source are an excellent alternative due to their low investment and operating costs and scalability to many industrial applications, and also due to the measured plasma characteristics (low surface charging, broad energy distribution). The appreciable increase of adhesion by anode layer source plasma pre-treatment and the effects of ion energy and gas composition are presented for room temperature sputtered titanium nitride coatings polyamide, polycarbonate, and poly(ethyleneterephtalate). For these polymers, the oxygen-based functionalization (chain-scissoring and cross-linking) strongly influence the wetting behaviour and improve the adhesion by suppressing adhesive cracking at low scratching loads. Low O_2 contents in Ar–O_2 discharge of ~400 eV average ion energy lead to best coating adhesion.

1. Introduction

The adhesion of thin films on surfaces is influenced by various properties including substrate roughness and cleanliness, film stress and structure, and thermal/mechanical properties of the substrate and film. Thus, the choice of substrate and film materials as well as substrate pre-treatment and coating technique is critical for achieving highly adherent coatings [1–3]. While the materials are usually determined by the application, pre-treatment and coating techniques attach great importance in industrial coating practices.

The application of plasma and ion beams for pre-treatment has been successfully applied to improve adhesion of various PVD and CVD deposited coatings [4,5]. The gas glow discharge between two electrodes is the simplest method, but it has the drawback of limited process control in ion energy and current density (dose). In contrast, ion sources produce plasma and accelerate ions from it with electrostatic or electromagnetic forces. Ion sources provide independent control of energy and current over a much wider range. (1) Gridded ion sources produce plasma in a discharge chamber and using electrostatic grids to accelerate ions toward the non-biased work-piece [6], which charging is prevented by plasma neutralization with electron sources. Gridded sources provide a high degree of independent control of ion energy and current. The ion beam is mono-energetic, allowing the selection of specific ion energies for process optimization. Despite the maturity of gridded ion source technology, these instruments can have drawbacks in certain industrial processes due to the high degree of complexity in their assembly and required maintenance of their grid optics. (2) Alternatively, gridless ion sources offer an elegant solution to ion beam production with many fewer parts and reduced maintenance requirements. One type of gridless ion source is the anode layer source (ALS). To produce plasma, two cathode plates focus a magnetic field in the gap in front of the anode [7]. Unlike the gridded source, the resulting ion beam has a broad ion energy distribution. The accelerated ion flux draws electrons from the source plasma and is virtually self-neutralized. [8,9]. Without the hindrance of accelerating grids and multiple electron source components, this device is considerably more robust, easier to maintain, uses fewer consumables, and may be powered with a single power supply.

After plasma generation the crucial treatment step is the interaction of energetic ions with the solid surface. Macroscopically,

* Corresponding author. Tel.: +43 3842 81260 2305; fax: +43 316 8769 2305.
E-mail address: juergen.lackner@joanneum.at (J.M. Lackner).

0042-207X/$ – see front matter © 2008 Elsevier Ltd. All rights reserved.
doi:10.1016/j.vacuum.2008.06.006

the reduction of the surface contamination, roughening and chemical activation (e.g. by oxidation) are commonly observed effects [10]. Bases therefore are microscopic interactions between the plasma particles and the frontier surface atoms. In polymer substrates, both ion species are introduced (doping or chemical effect) and irradiation-induced defects are formed by interaction with high-energetic ions (radiation or defect effect). Generally, the radiation effect is triggered by UV photons >3.5 eV (<355 nm) allowing bond cracking and cross-linking. While this effect is missing for metals and ceramics, it predominates in polymers compared to any doping effect [11] because: (1) doping is an "end-of-track" phenomenon with generally very low ion concentrations while the radiation is emitted over the whole ion track and produces a high yield. (2) Breaking bonds of organic molecules results in an ensemble of smaller, partly volatile. (3) The ability to anneal out damage during implantation becomes progressively worse in the order of metals, inorganic insulators and polymers.

Based on the knowledge of these effects this study shows the influences of the ALS pre-treatment of three different technically widely-used polymers on the surface properties and subsequent coating adhesion.

2. Experimental

The linear ALS (ALS340L, Veeco Instruments Fort Collins, CO) [7] used for the pre-treatment of polymer substrates for sputter coating has a spectrum of ion energies ranging from nearly zero to the magnitude of the anode potential, which can generally be set in the range 0.7–3 kV. The mean ion energy is typically about 60% of the discharge potential (0.4–1.8 keV) with a typically beam current of 1–2 mA cm^{-2} directly over the plasma channel [7]. A unique feature of the Veeco linear ALS are sputter shields that drastically reduce iron contamination (<0.1%) and produce extra electrons for enhancing beam neutralization compared to other commercially available ALS designs [12]. The ALS is installed in the industrially-scaled *Hybrid* PLD deposition plant [13–16] at Laser Center Leoben. The technical quality polymer substrates (polyamide 6.6 (PA), polycarbonate (PC), polyethylene terephtalate (PET)) were mounted on the slowly oscillating (2.4 min^{-1}) substrate table after chemical cleaning. The equipment was subsequently pumped down to 2×10^{-5} mbar for performing the experiments.

The following strategy was set for the development of adhesive coatings: first of all, the ALS characteristics (floating potential, ion current) in controlled process atmosphere (Ar, N_2, O_2 gas flows) were determined on-line by Langmuir probe measurements in dependency on the lateral distance across the ALS beam and an optical spectrometer for plasma emission in the 250–1100 nm wavelength range (USB 4000, Ocean Optics Inc.). The next step was the ALS pre-treatment at different acceleration voltages and gas mixtures for a wettability optimization based on contact angles (distilled water, 20 °C, 1 μl droplet volume). Additionally, atomic force microscopy (AFM) in tapping mode was performed for roughness and topography determination. These experiments were followed by an additional deposition of 5 and 50 nm thick interface layers, sputtered in Ar atmosphere at 1.4 kW at room temperature substrates from pure titanium targets for Fourier-transformed infrared spectroscopy measurements (FTIR, Perkin–Elmer Spectrum One) in attenuated total reflection (ATR) mode. Finally, on top of the interface layers titanium nitride (TiN) coatings with varied thickness were sputtered at room temperature in reactive Ar–N_2 atmosphere for adhesion testing (CSM Micro Scratch Test, HRC diamond indenter with 200 μm tip radius, 20 mm/min scratch speed between 30 mN–30 N) and for tribological pin-on-disc tests (Al_2O_3 pin, 2 N, 2000 turns).

3. Results and discussion

3.1. Characterization of the ALS plasma under polymer pre-treatment conditions

Based on the experience operating the ALS, the pre-treatment parameters were kept in a range of low charging of the insulating polymer substrates. This is reached by gas pressure and reactive gas flow control, the latter shown in the following with gas compositions consisting of Ar, O_2, and N_2 applied in discharge voltages between 1 and 3 kV (full working field of the ALS).

As expected, the electron density in the ALS discharges was found to be generally 1–3 orders of magnitude higher than the ion arrival rate in the formed plasma, measured by Langmuir probe measurements in 120 mm distance to the plasma channel, which is an average working distance in the applied sputter coating machine. Ion arrival rates on the substrate surface in such distance are in the range of 5×10^{12} mm^{-2} s^{-1} for 3 kV Ar discharges on a static (non-turning) position (Fig. 1). These arrival rates decrease to about half for 2 kV and to about a third for 1 kV discharges, the lower threshold for steady working with the ALS (plasma breakdown at ~0.8 kV discharges). Mixing oxygen and argon leads to increasing ion arrival rates up to $\sim 8 \times 10^{12}$ mm^{-2} s^{-1} for O_2/Ar gas flow ratios up to ~1. At higher ratios (and in pure oxygen) a decrease to $\sim 6 \times 10^{12}$ mm^{-2} s^{-1} is visible. A similar, slightly weaker tendency was found for discharges in Ar–N_2 atmospheres.

The floating potential from ground is generally decreasing by N_2 or O_2 mixing to Ar at constant total gas flow (for 3 kV discharges shown in Fig. 1). Lower energy (i.e. lower anode potential) working conditions increase the floating potential for the N_2 and O_2 gas mixtures, but scarcely influence the relatively high floating potentials amplitudes seen in pure Ar, which is about +11 to 13 V with respect to the system ground potential. An increase of averagely 2 V was found for 1 kV discharges in Ar–O_2 and O_2 compared to the 3 kV anode voltage, while the floating potential is nearly doubled in the N_2 discharge at 1 kV. This trend in floating potential relates to the typical increase in effective electron temperature that one observes when mixing molecular gas with Ar. While the plasma potential above ground does not strongly vary with input gases' conditions, the plasma potential to floating potential increases as a function of effective electron energy or temperatures [17].

To lowest order the difference between the plasma potential and floating potential at an electrically floating boundary may be estimated by

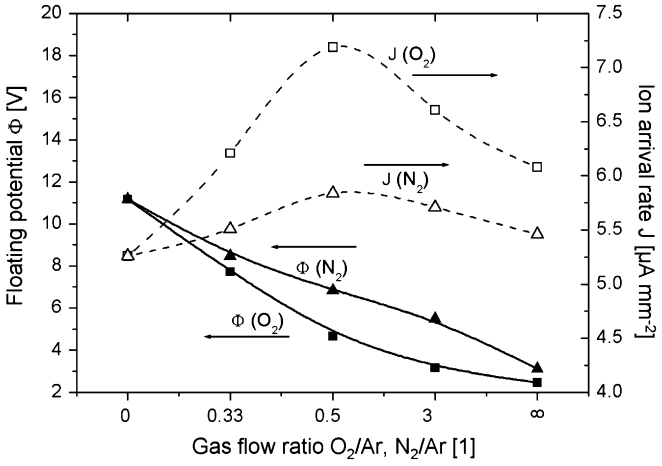

Fig. 1. Floating potential and ion arrival rate on a substrate surface for ALS plasma for various Ar–N_2–O_2 gas flow ratios at 3 kV discharge voltage.

$$V_F = -T_e \ln\left((M_i/2\pi m_e)^{0.5}\right) \quad (1)$$

where T_e is the apparent electron temperature in the ion beam plasma and M_i and m_e are the ion and electron mass. This expression accounts for ion and electron arrival rates but does not account for secondary electron emission currents which may be as high as 10–20% of the ion beam flux depending on the target materials.

It is a general observation in many plasma source systems that Ar plasmas (and many easy to ionize gases) typically have apparent electron temperature values that are lower than that for O_2 and most other molecular gases and even for weak Ar:O_2 dilutions. Thus, one expects that the plasma to floating potential value, V_F, for Ar to be lower than that for O_2. Since our measurements of floating potential are reference to ground and not the plasma potential, we should expect that the measured potentials in Ar should yield a more positive value than that for O_2.

Investigating the lateral distribution of the floating potential and the ion density by Langmuir probe measurements allows an insight into the phenomena occurring in the plasma and additionally a more detailed understanding of the influence of substrate movement of the cleaning/activation effect by the ALS plasma. The measurements were performed on the normal substrate position 120 mm far from the ALS surface close to its centre, above the plasma channel and distances of 20 and 40 mm outside the plasma channel. Both floating potential and ion arrival rate are at peak values in the plasma channel position. Outside this peak area ($\sim$20 mm lateral expansion) the ion arrival rate is decreasing much faster than the floating potential for all gas mixtures (e.g. 25% ion arrival rate decrease and only 0.1 V floating potential decrease in 20 mm distance outside the plasma channel position). Together with the general low difference between floating and plasma potential, it seems that this drop in ion arrival rate is mainly due to ion beam divergence, and loss of energy to the background gas through scattering and charge exchange outside the small region of the expanding ion beam above the plasma channel. These findings are in close connection to complex SRIM simulations (Stopping Range of Ions in Matter [19,20]) including the gas flow through the ALS. They showed an ion distribution in front of the ALS shaped like an elongated plasma torch with the highest ion arrival rates in its centre and decreasing outwards and with higher distance to the plasma channel.

Plasma emission measurements strengthen the findings of ion arrival rates for Ar and O_2 plasma. The strongest emission is found in the near-UV range ($\sim$4–6 eV photon energy) and between 600 and 900 nm (1.4–2 eV photon energy) originating from the excitation of neutral gas species (Ar^I and O^I transitions, plasma emission lines taken from Ref. [18]). The emission in nitrogen discharges is significantly lower than the Ar and O_2 emission. The main emission lines (peaks) found are in the range of 250–255, 384–387, 446–450, 614–618, 670–674, 775–780, and 843–846 nm for oxygen (O^I transitions), 349–352, 376–380, 695–698, 705–708, 736–739, 749–753, 770–774, 799–803, 810–813, and 825–828 nm for argon (Ar^I transitions), and 313–316 (N^{II} transition), 687–694, 816–823, and 866–870 nm for nitrogen (N^I transitions). Due to the extremely high light emission of the neutral species – comparable to a glow discharge – emission lines of ions in the plasma are hardly visible in the spectra taken in 50 mm distance to the plasma channel. This observation correlates with low electron energies seen within the downstream ion beam by the Langmuir probe measurements noted above. Increasing the O_2 concentration in the O_2/Ar gas mixture yields a linearly proportional increase in O_2 species emission. Higher anode voltages and, thus, higher energetic ions results in more intense photon emission from excited neutral species (background gas), however, additional emission lines of other excitation levels at higher threshold energies are missing.

Concluding the plasma observations, the high-energetic ions in the ALS beam lead to strong excitation of the gas in the recipient atmosphere by ion-neutral collision and scattering rather than by localized electron excitation activity in the downstream region of the ion beam. SRIM simulations of Ar ion scattering in neutral Ar background gas reveal this by two facts. Firstly, the high-energetic 100–1000 eV Ar ions reaching the substrate surface in 120 mm distance to the emission lose averagely 15–25% of their initial energy. Secondly, this "lost" energy is transferred by excitation/ionization of the background Ar gas, resulting in averagely $<$30 eV photon and ion energy. Finally, a 1000 keV primary ion can excite e.g. up to 50 near-UV photons (5 eV) or up to 100 (2.5 eV) visible-light photons. Consequently, the ALS plasma at the substrate surface consists predominately of low-energetic activated species of $<$30 eV and some additional slightly scattered, but still high-energetic species.

Together with the low-energetic plasma (10–30 eV) species, which is implanted and lead to chemical reactions, cross-linking and functionalization, this high density of 2–6 eV photons is highly advantageous for cleaning and activating polymer surfaces [22]. Compared to the few published works about polymer activation with ions $<$1 keV providing data of ion doses (e.g. [19,21]), the high, but spatially limited ion density of the ALS ($\sim$80 mm width in 120 mm substrate distance) in the range of 5×10^{12} mm^{-2} s^{-1} in the peak region is optimally suitable for polymer surface activation. By applying either substrate rotation (which is generally necessary for coating larger specimen) or/and by adjusting the treatment time (as shown in the following) ion doses of 10^{13} to 10^{14} mm^{-2} are easily possible with $\sim$10 s plasma treatment time. By the presence of electrons in the plasma charging of the surface is minimized and the polymer surface is slightly heated [22]. The small fraction of higher energetic ions (100–1000 eV) can etch the surface by sputtering, but lead also to chain-scissoring (polymer degradation) and deep implantation [22,23].

3.2. Contact angle modifications by ALS plasma treatment

Based on the determined ALS plasma characteristics short-time treatments (1 and 3 min total treatment time with $\sim$10 and $\sim$30 s total, but intermittent exposure to the ALS plasma, respectively) were performed on the polymers to gather the surface wetting behaviour as a basis for subsequent coating development. Thus, ion doses of $\sim 6 \times 10^{15}$ and $\sim 2 \times 10^{16}$ mm^{-2} are achieved. Limitation of ion doses resulted from preceding investigations of poly(methyl methacrylate) (PMMA) substrates revealing polymer degradation by a formation of amorphous carbon networks by a antireflection (moth eye) effect [24].

First of all, the water contact angle is decreasing for all three characterized polymers (PA, PC, PET) after all ALS treatments. The effect is as higher as lower the discharge anode voltage is (Fig. 2a) due to lower roughening found in AFM investigations ($R_a \sim 30$ and 35 nm for 1 and 2 kV treatments of PC) and possibly different chemical changes. Longer treatment (3 vs. 1 min) results in further slight decrease for PA and PC ($<$15% of the change between untreated and 1 min treated samples), while the contact angle remains constant for the PET samples for the 3 min treatment time. The roughening is in all cases orders of magnitude lower as shown by Capps et al. for PTFE [25] (treatment time and ion dose is not given in this work). As well known for all other plasma treatment techniques, the low contact angles are only a temporary effect (Fig. 2b) increasing to a stable level after several hours of storage in air atmosphere.

The next step was set by the variation of the gas composition at the low-energetic treatment condition (1 kV, 1 min treatment time with 10 s intermittent expose to the ALS plasma) to determine the influence of oxidation and substrate charging (see Fig. 1). As seen in

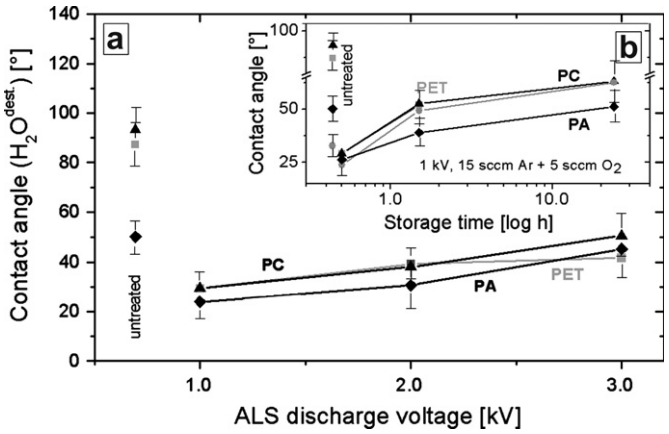

Fig. 2. Influence of the anode discharge voltage on the contact angles of PET, PA, and PC surfaces (a) immediately after the ALS plasma treatment (1 min treatment time with totally ~10 s intermittent expose to the ALS plasma, O_2/Ar gas flow ratio = 0.33) and (b) after storage in ambient air atmosphere (20 °C, 50% relative humidity).

Fig. 3a, lower contact angles were not achievable both for higher and lower gas flow ratios. Even the increase of the treatment time results in no significant decrease in the contact angles. Thus, the surface seems saturated with oxygen in the ALS plasma with O_2/Ar gas flow ratio = 0.33 by comparing to the findings of Egitto [20]. The sputtering effect of Ar ions seems to cause the roughening of the samples (see Fig. 3b for PC) treated in pure Ar, while for the low O_2 containing mixtures showing the lowest contact angles a distinct smoothing is found compared to untreated PA samples. However, pure O_2 treatments results again in higher roughness. Additionally, the AFM show for the Ar treated surfaces larger sized surface topography, which are decreasing in their size with increasing O_2 gas mixing, but increasing in their density – possibly an effect of sputtering by Ar and oxidation by O_2.

3.3. Chemical adhesion mechanisms of metal coating on ALS pretreated surfaces

Measured contact angles of plasma treated surface can only give hints about the condition of a polymer surface for subsequent coating. Thus, detailed chemical studies are necessary for the understanding of the chemical adaptation of the polymer by the plasma treatment. In the case of any subsequent thin metal coating, the density and strength of metal–polymer bonds are decisive for the adhesion of the film, because strong surface roughening would depict in unintended topography modifications for the (some micrometers thick) thin film and, thus, in mostly worse optical, mechanical, electrical, etc. properties.

To understand the binding of thin sputtered titanium interface layers (5 and 50 nm thick) on ALS plasma treated PC, PA, and PET surfaces, FTIR-ATR measurements were performed. For the manufacturing of the samples 1 kV discharge voltage, 0.33 O_2/Ar gas flow ratio, and 1 min treatment time (10 s intermittent expose to the ALS plasma), allowing quite low contact angles, were chosen in order to prevent any plasma over-exposure of the samples. The FTIR-ATR method allows a very surface sensitive evaluation (up to 0.5–1 μm depth) of the chemical binding at even coated polymer surfaces, e.g. see Ref. [26]. Assigning the FTIR peaks to the distinct changes in the polymer chains enables the detection of stretching and bending of organic (and inorganic) bonds. Fig. 4 shows the generally found spectra for the ALS treatments with O_2 presence, which are nearly independent on the gas mixture. Comparing all spectra of sputter coated and ALS pretreated polymers with the virgin, untreated one's, weakening of the reflected light due to the covering metal layer is evident, becoming higher for the thicker Ti films. Although the weaker peaks complicate the analysis, several additional features are present. First of all, all coated polymers show reflectance bands between 1800 and 2400 cm^{-1} light shift resulting from mainly C=C (up to 2200 cm^{-1}) and possible C=N binding [27–29]. The ~2350 cm^{-1} peaks can be due to CO_2 in the polymer surface or from atmospheric CO_2 during the FTIR measurement, although a CO_2 correction was done. Additionally, PET and PC show a slight decrease in C–H bonds (1350–1470 cm^{-1}) due to H scissoring (or bending of C–H) in alkanes [28], and PA shows a decrease in C–H stretching (~2850 cm^{-1}). Finally, some indications for less C=O bonds are evident for all investigated polymers by the higher reflectance around 1730 cm^{-1}. Definitely,

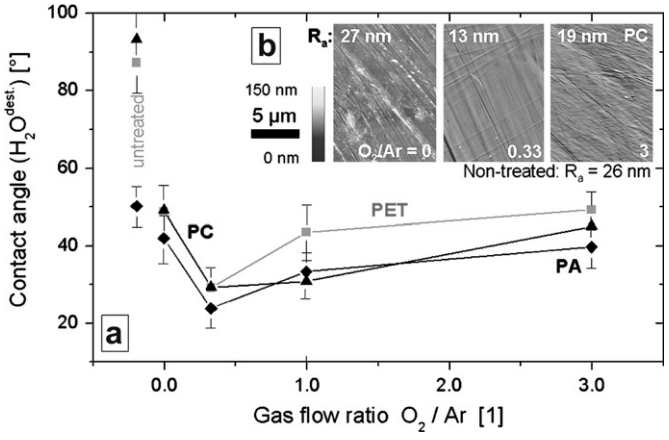

Fig. 3. (a) Contact angles of PC, PET, and PA in dependence on the O_2/Ar gas flow ratio in a 1 min treatment time, 10 s intermittent expose to the ALS plasma, 1 kV ALS plasma discharge. (b) Effects on the AFM measured surface topography and roughness for PA samples.

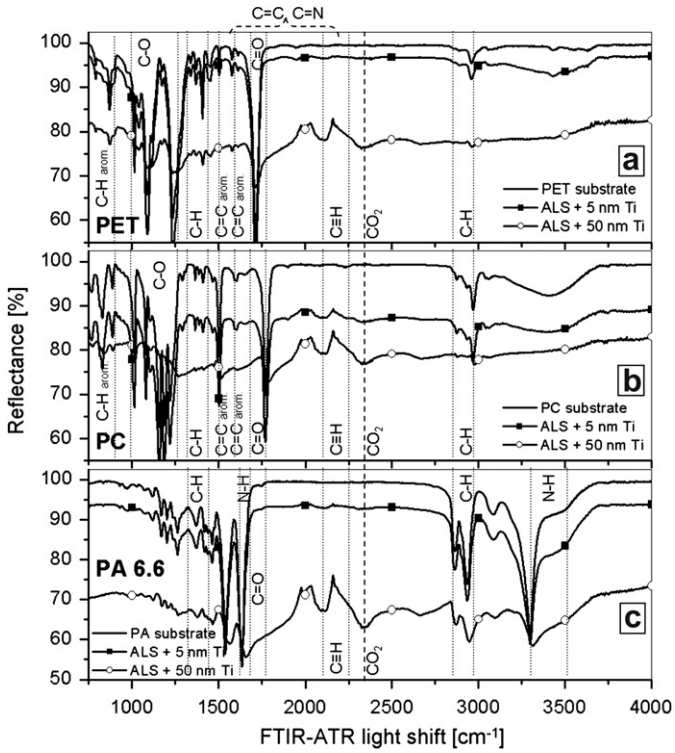

Fig. 4. FTIR-ATR reflectance spectra of PET, PC, and PA, untreated and ALS plasma treated with 5 and 50 nm Ti adhesive interface layers (ALS treatment: 1 kV, 1 min treatment time, 10 s intermittent expose to the ALS plasma, O_2/Ar = 0.33 gas flow ratio).

cyclic TiC_3 compounds are not present at the interface (vibrations at ~624, 1484, and (weak at) 573 cm^{-1}) [30].

Before concluding these FTIR findings, the general mechanisms of degradation (random chain-scissoring) and polymerization (cross-linking) should be addressed for the polymer groups. Chapiro [23] concludes that depending on the polymer material and its structure, one mechanism may prevail. Generally, the polymer cross-links under the influence of (near-)UV photons, if the structure of a vinyl polymer is such that each carbon atom of the main chain carries at least one hydrogen atom (like in polyethylene (PE), polypropylene (PP), polystyrene, poly(vinylchloride), polyimide, and also in PA, PET). Alternatively, if a tetra-substituted carbon atom is present in the monomer unit, the polymer degrades (e.g. poly(tetrafluoroethene) and also PMMA (see moth eye effect earlier) and PC). This empirical finding can be explained by the fact that the carbon bond in the main chain is weakened by the presence of the tetra-substituted carbon atom since they cause a strain in the molecule by a steric repulsion effect [23]. Based on the theoretical model of Kondyurin et al. [31] degraded layers are extending 1–100 nm below the surface. Due to the coexistence of cross-linking and degradation, cross-linked are generally found below the degraded layer expanding up to 100 nm thickness.

Having additional reactive oxygen species in plasma an oxidized polymer layer (<1–10 nm thick) is formed on top of the polymer during the plasma treatment [31]. Therein, the oxygen atoms are found either in the main polymeric chains or in hydroxyl groups. As higher the content of oxygen in the main chains is, as higher the tendency for binding of the chains to e.g. plasma deposited metallic atoms is. Polyolefines (e.g. PE, PP) have rather no polar functional groups and adhesion-improving pre-treatment is necessary to introduce these polar atoms (O, N) or functional groups into the chains. If ester group (polyesters: e.g. PET, PC, PMMA) or amide group (e.g. PA) are within the main chain, plasma first attacks the most polar bonds [32]. Thus, existing functional groups can be easily destroyed by plasma or transformed into simple hydroxyl groups (–OH) and new bonding sites have to be introduced for binding to metal atoms [33].

Comparing these general rules to the ALS treated polymers, the decrease in C–H bonds and the increase in C=C bonds are indications for cross-linking in the polymer surface (surface sensitivity of FTIR: 0.5–1 μm below the polymer surface), triggered by near-UV photons. The degradation of PC can possibly be observed in the very weak C–O band (1000–1260 cm^{-1}) found mainly for the ALS treated PC sample with 50 nm Ti interface layer.

Nevertheless, also the question regarding Ti atom to polymer chain binding can partly be solved by the FTIR analyses: C=O binding (1670–1760 cm^{-1}) is decreasing for ALS treated and coated PC and PET, while for PA a shift of the N–H assignable band (1580–1650 cm^{-1}) to higher wave numbers is present – possibly indication also N–O binding (band at 1500–1660 cm^{-1}). Thus, oxygen atoms introduced by the ALS plasma seems to form covalent binding (C–O–Ti, N–O–Ti) sites for the oxygen-affine titanium atoms. As higher the covalent binding character between these oxygen atoms and the metal deposit is as stronger the bonding is [34]. Such mechanisms – Ti–O bonds – were found in X-ray photoelectron spectroscopy depth scans of titanium coated polyurethanes too [16].

3.4. Adhesion and tribological behaviour of sputtered TiN coatings on ALS pretreated polymers

Applying the knowledge about minimizing contact angles and binding mechanisms on the design of a tribological coating resistant against scratch and sliding wear on PC, PA, and PET was the final goal of this work. Therefore, besides the optimization of the ALS plasma treatment for highest possible adhesion the optimization of the TiN film and Ti interface thickness is decisive. First of all, ALS plasma treatments in pure Ar atmosphere lead to weak adhesion of the coatings, partly with delamination already during coating, which is only slightly better than the adhesion of coatings without any plasma treatment. In contrast, mixtures of oxygen and argon were highly advantageous for PET, PA, and PC samples due to introduction of functional O binding sites (see above). Generally, the lowest adhesion was found for PA surfaces, which was therefore chosen for the following discussion.

While ~5 times higher critical scratch loads were found for PET and PC by comparing coated non-ALS treated and Ar–O_2 plasma treated samples, testing of PA yielded only ~4 times higher critical loads. However, the influences of TiN film and Ti interface layer thickness acting as load support are best visible for PA (Fig. 5b). Increasing the Ti or TiN layer thickness leads inevitably to higher critical loads (higher scratch resistance) largely influenced by the layer thickness, thus the load support is critical if the binding Ti polymer is optimized. Depositing TiN without any interface layer directly on the ALS treated samples results due to both the lower elasticity and plasticity of the TiN layer and – possibly – chemical effects to decisively lower critical loads. Based on the dependency found for the 2 μm TiN it seems that a gradient coating design of increasing elasticity promotes the load support additionally by possible shearing in the softer interlayer. This was proved by finite element simulations (Elastica 3.0 [35]) too.

Under the applied scratching load cracks in the film in the scratch track area are common, starting at 2–5 N loading. These cohesive cracks (for cracking mechanisms see Ref. [36]) are due to the very different elastic properties of polymers (~5 GPa) and coatings (~100 and 200 GPa for Ti and TiN) and are not critical because of the missing of any further crack propagation along the interface or a sub-surface weak-layer in the polymer. In contrast, the non-pretreated samples show a large scale tendency to cracking in the latter mentioned regions leading to adhesive failure in and in the surrounding of the scratch tracks. This seems to be due to the missing of surface functionalization by the introduction of functional groups due to the presence of oxygen during plasma treatment. Similar effects seem to lead to the worse behaviour of the polymer with ALS plasma treatment in Ar.

Fig. 5a shows in correlation to the adhesive improvements the results of pin-on-disc wear testing on ALS plasma treated and Ti-TiN coated PA. Two regimes are present: low wear is found for the thicker TiN films with Ti interface layers, in which high critical loads were determined, high wear for easier delaminating thinner films and missing Ti interfaces.

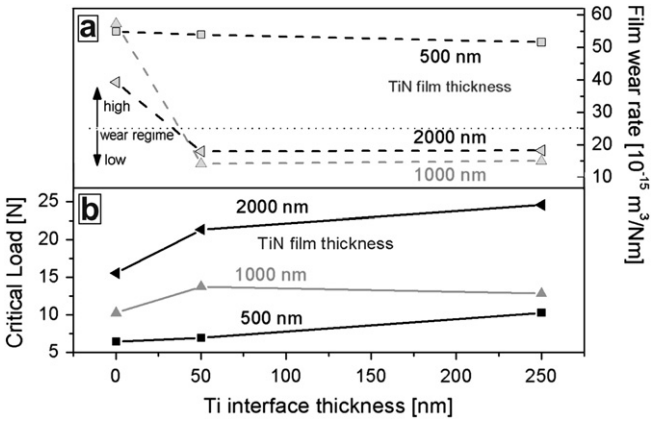

Fig. 5. (a) Film wear rate in pin-on-disc testing (Al_2O_3 counterpart pins, 2 N load, $N = 2000$) and (b) critical scratch test loads (HRC diamond intender) for ALS pretreated (O_2/Ar gas flow ratio = 3, 1 kV, 1 min treatment time, 10 s intermittent expose to the ALS plasma) and sputter coated PA surfaces in dependency on the Ti interface layer and TiN top coating thickness.

4. Conclusions

The ion and plasma treatment (e.g. by glow discharges) is a state-of-the-art technique for improving the film adhesion in industrial vacuum coating, although major problems exist in the application for temperature-sensitive and/or electrical non-conductive materials like polymers. To overcome these problems, gridless ion sources (like the anode layer source) were developed in recent years, presenting a robust alternative for industrial applications due to their simplicity in construction and use as well as their easy scale-up. In the current work technical grade PC, PA, and PET were pretreated by an ALS in different $Ar–O_2–N_2$ gas mixtures and coated by sputtering of Ti and TiN thin films for increasing the scratch and sliding resistance of the polymer surfaces. The main feature of the ALS is its linear scalability and the use of reactive gas mixtures at low substrate charging. Contact angle measurements after very short treatment times showed a strong decrease of the contact angle mainly in O_2–Ar gas mixtures of low O_2 content. The functionalization of the polymer chains with oxygen atoms for binding to metal Ti interfaces, proved in surface sensitive chemical studies, is decisive for achieving strong adhering TiN top coatings.

Acknowledgements

The financial support for this work was granted by the Austrian Federal Ministry of Traffic, Innovation and Technology (BM VIT) in the frame of the Research and Technology Focus Program of the Austrian Federal Government, by the Austrian Research Funding Organization (FFG) in the frame of the Austrian Nanoinitiative programme, by the Styrian Government, and by the European Union in the frame of the EFRE programme. The authors thank the companies Veeco Instruments Inc. (Fort Collins, CO/USA) and veonis Technologies GmbH (München-Puchheim, Germany) for their technical assistance.

References

[1] Mann DA. Plasma modifizierung von kunststoffoberflächen zur haftfestigkeitssteigerung von metallschichten, IPA-IAO Forschung und Praxis, Band 189. Berlin: Springer; 1994.
[2] Vallon S, Brenot R, Hofrichter A, d'Drevillon B, Gheorghiu A, Senemand C, et al. J Adhes Sci Technol 1996;10:1313.
[3] Vallon S, Hofrichter A, Guyot L, Drevillon B, Sapieha JEK, Martinu L, et al. J Adhes Sci Technol 1996;10:1287.
[4] Petasch W, Räuchle E, Walker M, Elsner P. Surf Coat Technol 1995;74-75:682.
[5] Haack RP, Smith T. Int J Adhesion Adhesives 1983;1:15.
[6] Harper J, Cuomo J, Kaufman H. J Vac Sci Technol 1982;21:737.
[7] Burtner D, Blacker R, Keem J, Siegfried D, Wahlin E. Proc 46th Ann Tech Conf Soc Vac Coaters 2003:263.
[8] Zhurin VV, Kaufman HR, Robinson RS. Plasma Sources Sci Technol 1999; R1:8.
[9] Keem JE. Proc 44th Ann Tech Conf Soc Vac Coaters 2001:388.
[10] Rank R, Wuensche T, Fahland M, Charton C, Schiller N. Proc 47th Ann Tech Conf Soc Vac Coaters 2004:632.
[11] Venkatesan T, Calcagno L, Elman BS, Foti G. In: Mazzoldi P, Arnold GW, editors. Ion beam modification of insulators. Amsterdam: Elsevier; 1987. p. 301–79.
[12] Burtner D, Siegfried D, Blacker R, Alexeyev V, Keem J, Zelenkov V, Krivoruchko M. U.S. Patent Appl 20050040031.
[13] Lackner JM, Waldhauser W, Heinz W, Brandstätter E, Schwarz M. Jahrbuch Oberflächentechnik 2007:115.
[14] Lackner JM, Waldhauser W, Schwarz M, Mahoney L, Burtner D. Proc 50th Ann Tech Conf Soc Vac Coaters 2007:87.
[15] Lackner JM. Surf Coat Technol 2005;200:1439.
[16] Lackner JM. Industrially-scaled hybrid pulsed laser deposition at room temperature. Krakow: OREKOP; 2005.
[17] Lieberman M, Lichtenberg A. Principles of plasma discharges and materials processing. New Jersey: Wiley; 2005. p. 172.
[18] Payling R, Larkins PL. Optical emission lines of the elements, Software Version 1.6.1. London: Wiley; 2000.
[19] Ziegler JR, Biersack JP, Littmark U. The stopping and range of ions in solids. New York: Pergamon; 1985.
[20] Ziegler JR, Biersack JP. SRIM – the stopping and range of ions in matter. Software-Version 2006.02; 2006.
[21] Lee JH, Cho J-S, Koh S-K, Kim D. Thin Solid Films 2004;449:147.
[22] Egitto FD, Matienzo LJ. IBM J Res Dev 1994;38(4):423.
[23] Chapiro A. Radiation chemistry of polymeric systems. London: Interscience; 1962. p. 354.
[24] Unpublished results, private communication to Mr. Stöckl, Fraunhofer IOF Jena (Germany).
[25] Capps N, Carter D, Roche G. Semiconductor Int 2000:7.
[26] Lackner JM, Waldhauser W, Schöberl T. Surf Coat Technol 2006;201:4037.
[27] Haag S. Ion beam assisted deposition of thin films in the system Ti-B-C-N und their characterization. Ph.D. thesis, University of Heidelberg; 2003, p. 143.
[28] Lin-Vien D, Colthup NB, Fateley WG, Grasselli JG. The handbook of infrared and raman characteristic frequencies of organic molecules. San Diego: Academic Press; 1991.
[29] Kimm F. Untersuchung der Konstitution sowie der mechanischen und optischen Eigenschaften magnetron-gesputterter c-BCN-Filme. PhD thesis, University of Karlsruhe; 1997.
[30] Kinzer RE, Rittby CML, Graham WRM. J Chem Phys 2006;125:074513.
[31] Kondyurin A, Gan BK, Bilek MMM, Mizuno K, McKenzie DR. Nucl Instr Meth Phys Res B 2006;251(2):413.
[32] Gröning P, Kuttel OM, Collaud-Coen M, Dietler G, Schlapbach L. Appl Surf Sci 1995;89:83.
[33] Garbassi F, Morra M, Occhiello E, Barino L, Scordamaglia R. Surf Interf Anal 1989;14:585.
[34] Burger RW, Gerenser LJ. Proc 34th Ann Tech Conf Soc Vac Coaters 1991: 162.
[35] Finite Element Software Package Elastica 3.0.. Radeberg: ASMEC; 2006.
[36] Bull SJ. Surf Coat Technol 1991;50:25.